

Ferric hydroxide and ferric hydroxysulfate precipitation by bacteria in an acid mine drainage lagoon

Wendy A. Clarke, Kurt O. Konhauser *, Julia C. Thomas, Simon H. Bottrell

Department of Earth Sciences, University of Leeds, Leeds LS2 9JT, UK

Abstract

The spontaneous precipitation of amorphous iron hydroxide and ferric hydroxysulfate has generally been considered to be an inorganic process involving the oxidation of ferrous iron with or without the presence of sulfate. However, our study of bacterial communities growing in an acid mine drainage lagoon sediment has confirmed that microorganisms were also capable of facilitating this mineral precipitation. Transmission electron microscopy revealed that bacteria growing at the surface had iron-rich capsules, along with detectable amounts of Zn, Ti, Mn and K incorporated into the mineralised matrix. In the subsurface, more cells were associated with granular, fine-grained mineral precipitates, composed almost exclusively of iron and sulfur. Pore water profiles indicated that no discernible sulfate reduction had taken place, suggesting that these authigenic minerals were ‘ferric hydroxysulfate’, and not iron sulfide. Energy dispersive X-ray spectroscopy further indicated that the subsurface minerals had variable composition, with the Fe:S ratio decreasing with depth from 3.5:1 at 15 cm to 1.9:1 at 30 cm. This indicates the high reactivity of ferric hydroxide for dissolved sulfate. Because iron reduction was limited to sediment depths between 3–10 cm, it is conceivable that these minerals are not amenable to bacterial reduction, and hence, the ability of bacteria to bind and form such precipitates may provide a natural solution to cleansing acidified waters with a high dissolved metal content.

Keywords: Ferrihydrite; Ferric hydroxysulfate; Bacteria; Biomineralization; Acid mine drainage

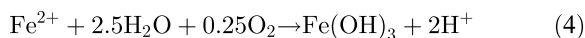
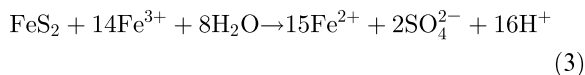
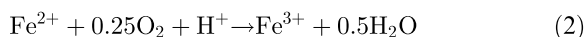
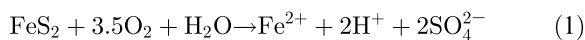
Contents

1. Introduction	352
2. Materials and methods	352
2.1. Sampling site	352
2.2. Laboratory analyses	353
3. Results	354
3.1. Surface and pore-water geochemistry	354
3.2. Solid-phase geochemistry	355
3.3. Microbial biomineralisation	356
4. Discussion	357
Acknowledgements	360
References	360

* Corresponding author. Tel.: +44 (113) 233-5225; Fax: +44 (113) 233-5259; E-mail: kurt@earth.leeds.ac.uk

1. Introduction

Amorphous ferric hydroxide (i.e. ferrihydrite), ferric hydroxysulfate and jarosite frequently occur as ochreous surface precipitates on stream beds receiving iron and sulfate-rich, acidic waters [1–6]. These minerals, with bulk compositions of $5\text{Fe}_3\text{O}_3 \cdot 9\text{H}_2\text{O}$ [7], $[\text{Fe}_{16}\text{O}_{16}(\text{OH})_{12}(\text{SO}_4)_2]$ [6] and $[\text{MFe}_3(\text{SO}_4)_2(\text{OH})_6]$, where M is one of several cations, including Na^+ , K^+ , and NH_4^+ [1], respectively, are often associated with areas receiving acid mine drainage (AMD). Generation of AMD results from the exposure and rapid oxidation of sulfide minerals associated with disused coal and metal mines. The general processes are outlined below [8]:



The first three reactions describe the initial abiotic or biotic oxidation of solid-phase sulfide (reaction 1), the subsequent microbial oxidation of Fe^{2+} under acidic conditions by *Thiobacillus ferrooxidans* (reaction 2), and the accelerated oxidation of metal sulfides by dissolved Fe^{3+} (reaction 3). When AMD comes into contact with fresh water at an off-site location, the oxidation and hydrolysis of Fe^{2+} (reaction 4) results in a voluminous yellow precipitate, characterised by its high reactivity in scavenging other metal cations from the effluent [9]. At low pH, ferric hydroxysulfate and jarosite precipitate through anion bridging of ferric iron colloids [2,4,6], while at higher alkalinity, in the absence of appreciable sulfate, the neutralising effects of relatively unpolluted stream water results in ferric hydroxide precipitation [10].

Although bacteria are directly involved in the oxidation of sulfidic minerals and the generation of AMD, their involvement in the subsequent precipitation of amorphous iron and sulfur phases is less clear. In an experimental study with isolates of *T. ferrooxidans*, Ivarson [1] observed that bacterial

oxidation of ferrous sulfate (in a liquid medium) accounted for the formation of jarosite, while growth on a solid medium of agar yielded ammoniajarosite ($\text{NH}_4\text{Fe}_3(\text{SO}_4)_2(\text{OH})_6$). Ivarson et al. [11] further recognised a relationship between the widespread occurrence of jarosite in nature with the chemical activity of *T. ferrooxidans*. These findings, in addition to further experimental study, prompted Lazaroff et al. [2] to suggest that bacterial processes somehow catalysed the production of the soluble precursors to ferric hydroxysulfates or jarosite, by lowering the activation energy barriers to their formation; under abiotic conditions different minerals formed.

Recent biomineralisation studies have shown the ability of bacterial cells to partition metals effectively from solution into sediments as authigenic mineral phases during the earliest stages of diagenesis [12–18]. The fixation of cations arises through electrostatic interaction with anionic carboxyl and phosphoryl groups on outer cell surfaces. Many cells are also surrounded by an extracellular sheath or capsule composed of polysaccharides, the molecular components of which are similarly reactive and consequently accumulate metals around the cell. Once metal immobilisation is achieved a special micro-environment is established allowing further growth of metal aggregates with the continued removal of ions from solution. Because biomineralisation must obey thermodynamic principles, the mineralised matrix that forms is generally composed of metal ions that are found in sufficiently high concentrations as to exceed their solubility products. In AMD, the concentrations of both iron and sulfate are relatively high. Subsequently, in this study we were interested in observing the role of bacterial communities, growing in an acid mine drainage sediment, in promoting the formation of iron-sulfur minerals.

2. Materials and methods

2.1. Sampling site

Tonmawr is a small village situated in the Afon Pelenna catchment area at the western edge of the South Wales Coal Field. The village has a long history of coal mining spanning a century; over 15 small drift mines and two larger mines developed

in the surrounding valleys working a number of coal seams in the Upper Coal Measures. Mining activity had ceased in the region by the early 1960s, leaving behind the ferruginous pollution caused by AMD. The Whitworth lagoon was constructed during reclamation of the Whitworth Colliery site in the mid-1970s by the then West Glamorgan County Council in an attempt to reduce the impact of two discharges (Whitworth A and B). The lagoon is approximately 300 m² in area and 2 m deep in the centre, with concrete sides. Water from two adits, which drain the surrounding spoil heaps, enter from opposite ends at the back of the lagoon, allowing the natural precipitation of iron-rich sediment. A small weir, 0.5 m in width, discharges the effluent into the Nant Gwenffrwd, a tributary of the Afon Pelenna, which is unpolluted above this point.

Sediment cores were collected within two metres of the settling lagoon embankment using 10 cm diameter core tubes. Immediately after the cores were removed from the water, sediment samples were extracted at 5 cm intervals using a sterile scalpel and placed into 2 ml metal-free plastic tubes containing 2% (v/v) glutaraldehyde, a fixative for electron microscopy. Additional sediment cores taken were frozen on-site using dry ice or stored at 4°C for 24 h before sectioning. Surface waters were analysed for alkalinity, pH and conductivity on location. Water samples were passed through Whatman 0.45 µm membrane filters to remove particulate matter; sub-samples were acidified on-site with 50% v/v nitric acid (to an acid concentration of 3% v/v) to prevent metal precipitation and placed in 30 ml Nalgene bottles. Both acidified and non-acidified samples were returned to the laboratory.

Pore waters were sampled using the conventional technique of centrifugation of sectioned sediment cores and polyacrylamide gel probes. The gel probes, based on the design and methodology of Krom et al. [19], measured dissolved anions (chloride and sulfate) and cations (iron and manganese). The gels were inserted into the lagoon sediment, close to the embankment and left to equilibrate for 6 h prior to removal. Once removed, the anion gel was immediately wiped clean before a central window was cut out with a sterile scalpel. The gel was placed onto a clean chopping board and quickly cut into 10 cm strips to minimise diffusion. The strips were then

sub-divided into 0.5 cm sections and placed into pre-weighed 1.5 ml metal free plastic tubes. The cation probes were immersed immediately in 10 mM NaOH for 4 h to 'fix' the metals within the gel as insoluble species. These cation gels were then chopped into 0.5 cm sections with a perspex cutter, and treated as above.

2.2. Laboratory analyses

Sedimentary cores were sliced into 2 cm segments, placed into 50 ml plastic tubes and centrifuged to extract pore waters. The supernatant was passed through Whatman 0.45 µm filters and sub-sampled into 30 ml metal free vials. The tubes containing anion gel slices were reweighed to obtain the gel mass. To each tube 500 µl Milli-Q water was added and left to re-equilibrate for 12 h. Both conventional and gel probe pore waters were analysed for dissolved sulfate and chloride using a Dionex DX 100 Ion Chromatograph with a 4 mm IONpac AS4A-SC column and a AS3500 auto-sampler and AI450 computer interface. Acidified surface and conventional pore waters were further analysed for dissolved metals using inductively coupled plasma-atomic emission spectroscopy (ICP-AES) at the Royal Holloway and Bedford College NERC Research Facility. The tubes containing cation gel slices were reweighed to obtain the gel mass. To each tube 200 µl 2 M HNO₃ was added and the tubes left overnight to allow remobilisation of the 'fixed' iron and magnesium. Samples were then diluted with 500 µl Milli-Q water and analysed using Graphite Furnace Atomic Adsorption Spectroscopy; a Varian Spectra 10, equipped with a GTA 96 Graphite Furnace was employed.

Bulk sediment mineral assemblages were determined by X-ray diffraction (XRD). Subsamples of the sediment were oven dried at 40°C and ground to a fine powder. Each sample was scanned from 4–70° using a CuαK radiator. Major and trace metals were analysed by X-ray fluorescence spectroscopy (XRF) using fused and pressed pellets. Using the leaching methods of Raiswell et al. [20], the reactive iron content of sediment was measured using dithionite and a hot HCl solution. The residue was filtered off and the remaining liquid analysed by atomic adsorption flame spectroscopy (Varian Spectra 10 GTA 96).

Sediment samples were prepared for thin sectioning by washing in a solution of 0.1 M phosphate buffer (pH 7.4), to remove excess glutaraldehyde, and post-fixed in osmium tetroxide (2% v/v). After washing, samples were dehydrated through a graded ethanol series and embedded in resin (Agar 100, Agar Scientific Ltd). Thin sections, approximately 60 nm thickness, were obtained with a Reichert-Jung Ultracut and mounted on collodion amyl acetate-carbon coated copper grids. To increase the electron contrast of cytoplasmic material of intact cells, thin sections were routinely stained with uranyl acetate and lead citrate before imaging in the electron microscope. Grids were viewed with a Philips CM 20 transmission electron microscope (TEM) operating at 200 kV, with a liquid nitrogen-cooled anti-contamination device in place at all times. Energy dispersive X-ray spectroscopy (EDS) (Link Analytical) was conducted using a beam spot size of 40 nm and by collecting counts for 100 s (live time). The d-spacings for crystalline mineral phases were examined by selected area electron diffraction (SAED), using a camera length of 620 nm. Elemental compositions of amorphous phases were characterised by EDS spot analysis.

3. Results

3.1. Surface and pore-water geochemistry

The dissolved sulfate profile showed a decrease in concentration from 750 mg/l to 500 mg/l within the top 4 cm of the sediment (Fig. 1A). The sulfate remained at a concentration of 500 mg/l to a depth of 12.5 cm, after which there was an increase to 750 mg/l, immediately followed by a decrease to 500 mg/l. Surface water concentrations were lower than pore water at 250 mg/l. The difference between surface and pore water concentrations was most likely due to recent dilution by rain water of surface water. The changes in concentration of sulfate within the pore water could be attributed to either: (i) sulfate reduction occurring in anoxic zones in the sediment, (ii) the interaction of sulfate with highly reactive, freshly precipitated iron oxy-hydroxides, or (iii) a dilution front caused by rain water moving down into the sediment. The profile of sulfate/chloride ratios with depth (Fig. 1B) indicated a constant ratio between the two species. This suggested that interaction with freshly precipitated iron oxy-hydroxides was the

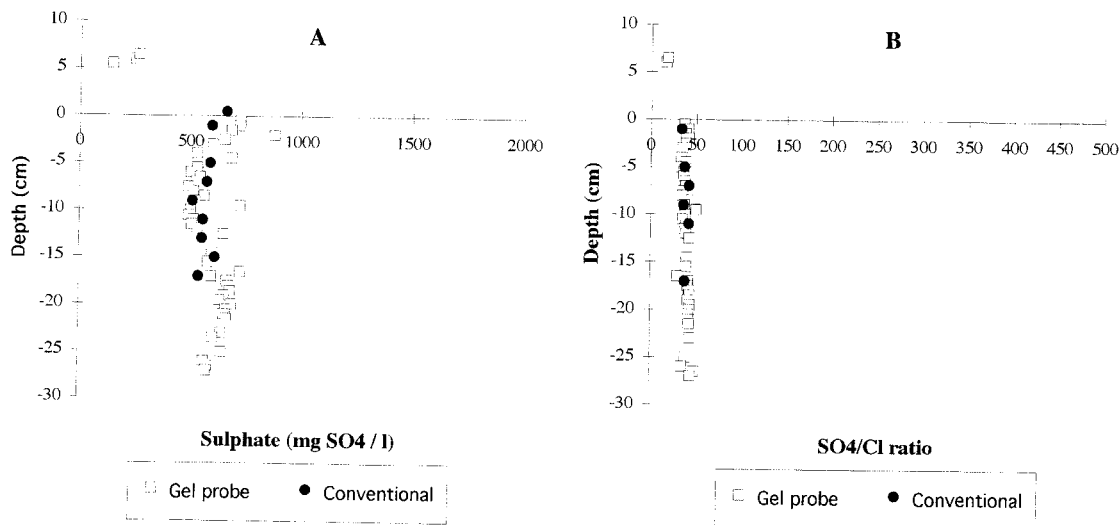


Fig. 1. Porewater profiles of (A) dissolved sulfate concentration versus depth in the Whitworth Lagoon sediment and (B) sulfate/chloride ratios versus depth.

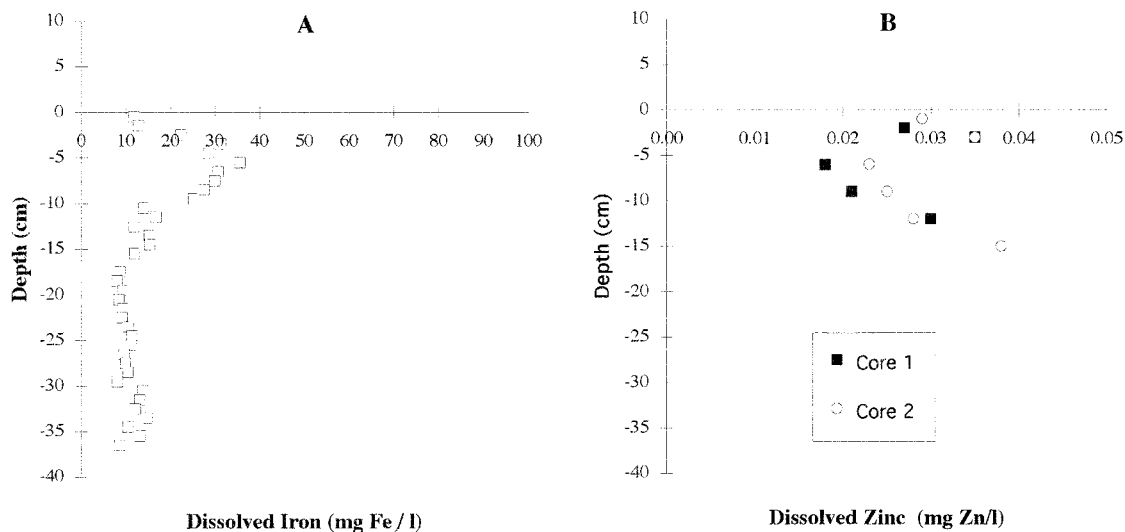


Fig. 2. Porewater profiles of (A) dissolved iron concentration versus depth in the Whitworth Lagoon sediment and (B) dissolved zinc versus depth.

most likely explanation for the depletion in sulfate concentration (possibly chloride is also bound). Conventional pore-water sampling concurred with these results.

The dissolved iron profile (Fig. 2A) showed that a large peak in concentration, from 10 mg Fe/l to 37.5 mg Fe/l, occurred at 3–10 cm depth, after which the concentration dropped to 10 mg Fe/l and remained constant until the base of the profile. The large increase was indicative of microbial reduction of Fe^{3+} to Fe^{2+} . Iron-reducing bacteria are known to readily metabolise amorphous iron hydroxides in preference to the more crystalline phases [21], which could account for the decrease in iron reduction with depth – as amorphous phases become more crystalline or as more sulfate is added to the precursor iron phases.

The profile of zinc concentrations within the pore water (Fig. 2B) is shown from two cores, both exhibiting similar trends. Near surface there are relatively high values of Zn^{2+} followed by a sharp decrease in concentration. This decrease may result from co-precipitation of zinc onto iron hydroxides and sorption onto bacterial surfaces. The concentration then follows an increasing trend to the base of the profile. The position of this increase in concentration corresponds to the zone of iron reduction, and indicates that zinc was being released into so-

lution when iron hydroxides were reduced. Unfortunately, Zn profiles were not obtained below a depth of 15 cm.

3.2. Solid-phase geochemistry

Visually all cores taken from the Whitworth Lagoon site consisted of bright orange-red fine grained sediment, with small (up to 1 cm diameter) localised patches of green and black material. Thin layers of detrital coaliferous material could be seen throughout the core, and thin sequences of hard red iron oxide crusts indicated past surface positions. The patches were normally found associated with plant material and were assumed to be reducing micro-niches formed around a labile carbon source. XRD traces indicated that all samples were dominated by amorphous iron(III) hydroxides. No crystalline iron minerals were identified. XRF analysis carried out on nine cores revealed that 40–70% of the sediment consisted of iron, 5–55% SiO_2 , 0–10% Al_2O_3 and 1–3% sulfur, with the remainder found at trace levels. Iron extractions to determine the highly reactive and poorly reactive phases of iron were then performed. The extraction with dithionite removed reactive iron phases: lepidocrocite, ferrihydrite, goethite and hematite. The HCl leach additionally removed the poorly reactive carbonate and silicate phases. Highly reac-

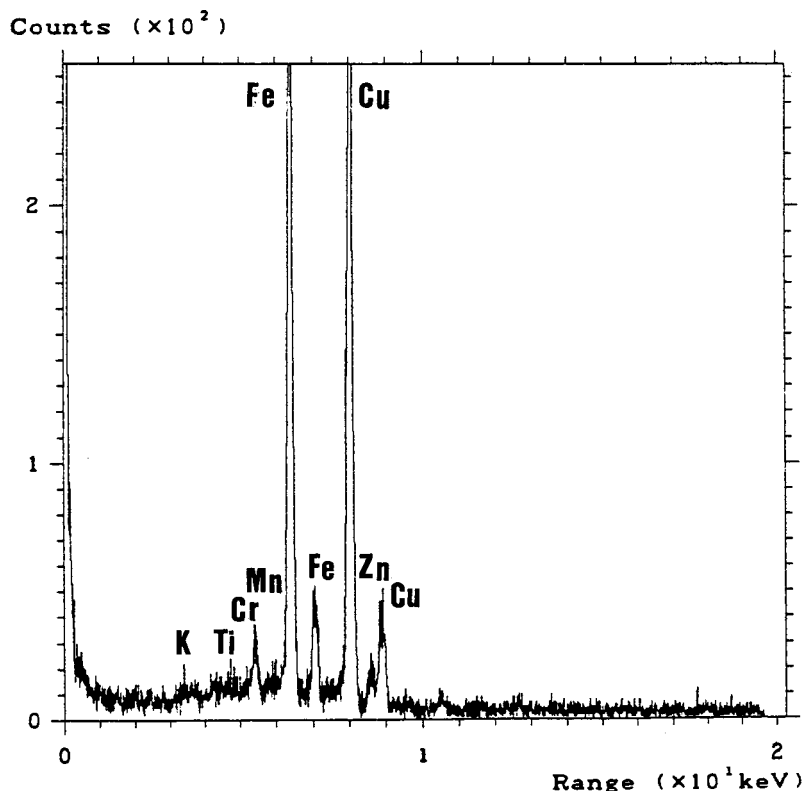


Fig. 3. EDS spectra of the mineralised capsule associated with bacterial cells at the sediment/water interface (0 cm depth). Cu peak from supporting grid and Cr is due to contamination.

tive iron in the sediment ranged from 46–52%, with only small amounts (0–2%) of poorly reactive phases. This indicated that the majority of iron on the lagoon was found as highly reactive amorphous phases. A small amount of the silicate and poorly reactive phases may be detrital shale fragments washed in from the surrounding spoil heaps.

3.3. Microbial biomineralisation

TEM analyses indicated that bacterial cells, collected from various depths (surface, 15 cm, 30 cm) served as nucleation sites for authigenic mineral precipitation. The biominerals ranged from mineralised capsules to fine-grained precipitates within the capsule and on the outer cell wall. Grain sizes for the individual precipitates were typically $< 0.2 \mu\text{m}$, and SAED indicated that the grains were amorphous in structure. In the surface samples, most cells appeared to have mineralised capsules, with the magnitude of

capsule material varying from individual cells to the encapsulation of microcolonies. EDS analyses indicated that the exopolymers sequestered significant amounts of Fe, as well as detectable quantities of Zn, Ti, Mn and K (Fig. 3). The binding of iron to cells is not surprising considering that the mine effluent contained 12 mg/l of the dissolved metal, and that iron is preferentially bound to organic sites due to its valency and hydration radius [22]. The accumulation of trace elements, such as Zn, which was found in low concentrations in the water (0.01 mg/l), indicated that the bacteria were also potent scavengers for other dissolved metals [14].

In the subsurface a greater proportion of bacterial cells had fine-grained precipitates associated with them, compared to only having mineralised capsules. The authigenic minerals appeared granular under the TEM (Fig. 4A), whereas others were completely encrusted in a dense mineralised matrix in which individual precipitates appear to have coalesced (Fig.

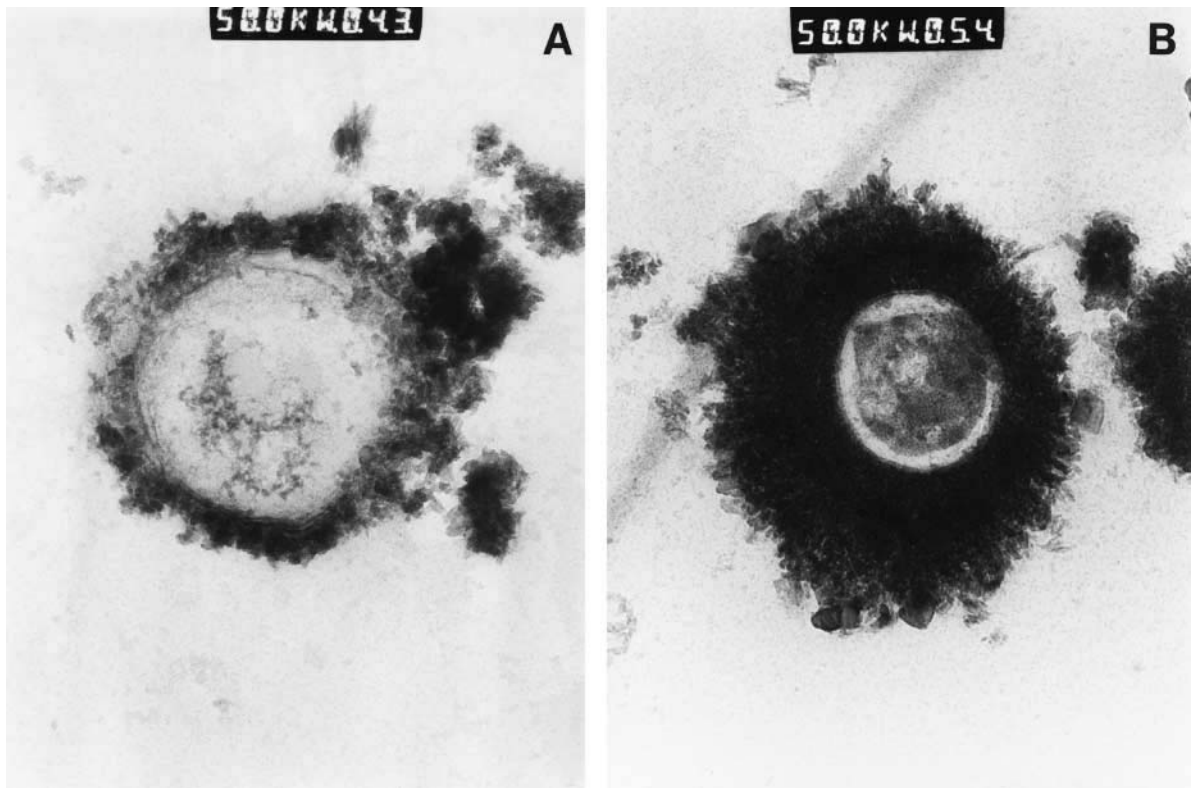


Fig. 4. Transmission electron micrographs of stained bacterial cells collected from sediments of the Whitworth Lagoon. A: Individual cell with fine-grained ferric hydroxysulfate precipitates on outer cell wall. B: Individual cell where ferric hydroxysulfate grains have coalesced into a dense, mineralised epicellular matrix. Micrographs are magnified 50 000 times.

4B). The former were more typical of precipitates at 15 cm depth, whereas the dense varieties were common at greater depths (i.e. 30 cm). The individual grains bear a striking resemblance in morphology and size to ferrihydrite prepared experimentally in the presence of a 250–1000 $\mu\text{g/ml}$ dissolved sulfate solution [4]. Not surprisingly, EDS of the lagoon bacteria indicated that these mineral phases consisted of an Fe-S complex with variable composition. As there was no observable sulfate reduction taking place, the authigenic mineral was tentatively described as a 'ferric hydroxysulfate' [4,6], and not iron sulfide. Furthermore, using atomic weight ratios, the Fe:S ratio decreased from 3.5:1 at 15 cm (Fig. 5) to 1.9:1 at 30 cm (Fig. 6) suggesting the continued reactivity of the ferric iron phase to dissolved sulfate ions (i.e. more sulfate reacts with previously formed ferric hydroxide with depth).

4. Discussion

The spontaneous precipitation of amorphous iron hydroxide and ferric hydroxysulfate has generally been considered to be an inorganic process involving the oxidation of ferrous iron with or without the presence of sulfate. However, in the Whitworth Lagoon, bacteria were found facilitating this mineral precipitation. The formation of epicellular iron hydroxides by bacteria can occur either passively or actively. In the first instance, the oxidation and hydrolysis of cell-bound ferrous iron or the binding of cationic colloidal species (e.g. $\text{Fe}(\text{H}_2\text{O})_5(\text{OH})_5(\text{OH})^{2+}$) can induce the transformation to insoluble hydroxide forms [14]. Alternatively, ferrous iron transported into an oxygenated environment spontaneously reacts with dissolved oxygen (at circumneutral pH) to precipitate rapidly as ferrihydrite (abiotically) on available nucleation sites. Bacteria merely

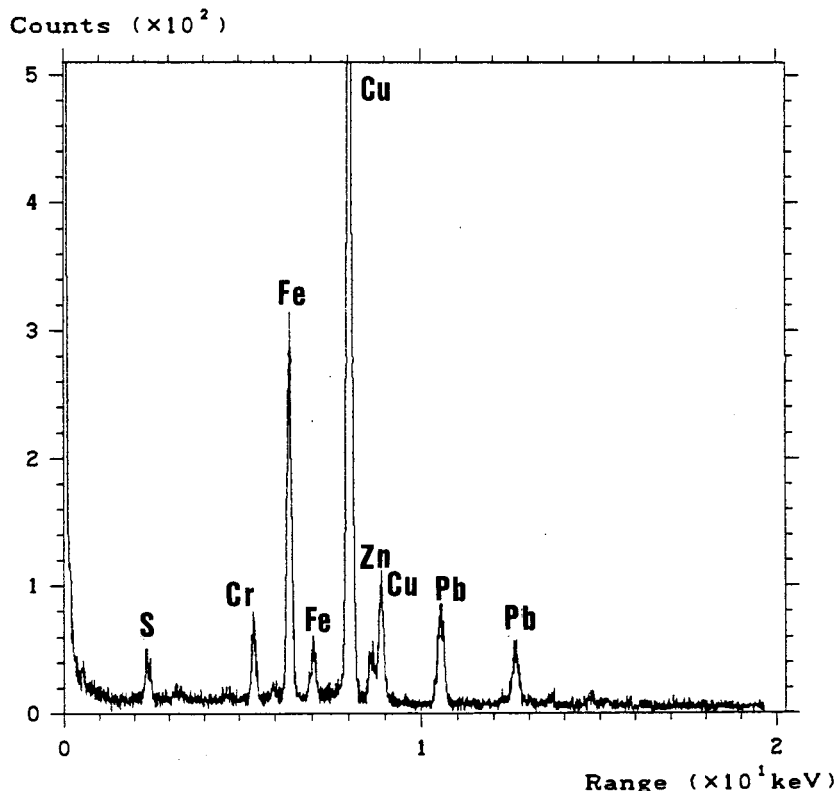
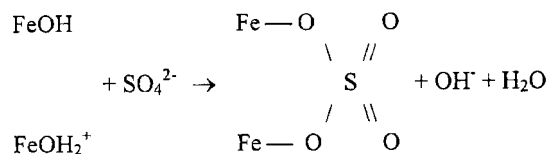


Fig. 5. EDS spectra of the epicellular mineral precipitates associated with bacterial cells at a depth of 15 cm.

represent such sites, and over a short period of time the microorganisms can become completely encrusted in amorphous iron. The second means by which iron hydroxides form stems from the ability of Fe(II)-oxidising bacteria to oxidise ferrous iron as an energy source. The activity of *T. ferrooxidans* not only causes the oxidation of metal sulfides under acidic conditions, but it may also promote iron hydroxide precipitation in aqueous environments where the pH allows for ferric iron to form an insoluble mineral [23].

Due to its amorphous structure, ferrihydrite is thermodynamically unstable, and with time will convert to more stable iron oxides, such as goethite and hematite [7]. Both oxides, however, were absent from all sediment samples. Synthesis experiments have shown that adsorption of small quantities of sulfate not only suppresses the ordering of ferrihydrite, but also hinders the formation of goethite and hematite [4]. Therefore, the incorporation of sulfate ions into the iron hydroxide matrix, as might be expected con-

sidering the high reactivity of ferrihydrite for counter-ions [24], and the high concentration of dissolved sulfate in the AMD sediment pore waters (550 mg/l), compared to dissolved iron (10 mg/l), may account for the presence of ferric hydroxysulfate minerals instead of ferrihydrite. A possible mechanism for sulfate adsorption onto iron oxides has previously been documented by Parfitt and Smart [25], who suggested that two hydroxyl groups are replaced by one sulfate ion. Binuclear bridging is then created when the two oxygen atoms of the sulfate ion are co-ordinated each to a different Fe^{3+} ion. This creates the complex $\text{Fe-O-S(O}_2\text{)-O-Fe}$ shown below.



Whatever the mechanism of formation, it was interesting to find that all the bacteria exhibited the

same biomineralisation with depth, implying that ferric hydroxysulfates are precipitated within the first few centimetres of the surface and subsequently buried with time. Significantly, because of the reactive nature of both ferrihydrite and ferric hydroxysulfates, additional trace metals may be incorporated into the mineral matrix via adsorption and co-precipitation [26]. This can be extremely important in controlling the levels of metallic ions released into AMD streams [9], presuming of course, that Fe(III) reduction does not re-mobilise them into solution.

The ability of bacteria to directly precipitate ferric hydroxysulfate may have important implications for microbial activity as a primary control in the remediation of AMD. For example, to improve water quality in these areas, artificial wetland treatment systems have been constructed with the purpose of providing a low-maintenance, self-generating biological system that increases effluent pH and concomitantly removes metals [27]. Several biological processes are suggested to improve water quality in

wetlands, including bacterial oxidation, metal uptake by plants and microorganisms, and metal precipitation as sulfide phases [28]. Studies of wetlands to date have shown that sulfate reduction and subsequent sulfide precipitation are more important processes for metal removal than the adsorption of metals onto organic matter [29]. Although organic substrates are added to wetlands to provide a carbon source for sulfate-reducing bacteria, and hence produce soluble sulfide for mineral precipitation, it has recently been observed that sulfate reduction rates decline within two years of construction, thereby releasing dissolved iron in the outflow [30]. The ability of microorganisms to bind and form iron sulfate minerals, however, may provide a natural solution to cleansing acidified waters with a high dissolved metal content. Although iron-reducing bacteria generate energy by coupling the oxidation of organic matter with the reduction of ferric hydroxide [21], their ability to reduce ferric hydroxysulfate is undetermined. Certainly, there is a clear lack of iron re-

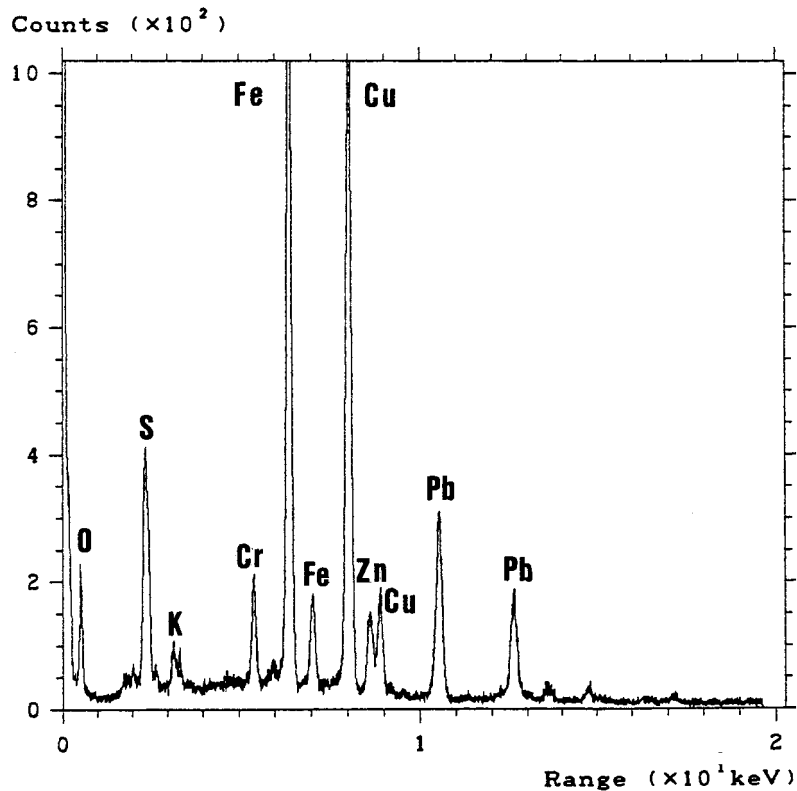


Fig. 6. EDS spectra of the epicellular mineral precipitates associated with bacterial cells at a depth of 30 cm.

duction below 3–10 cm, the depth at which iron sulfate minerals are formed. Whether this is a mere coincidence, or simply a reflection of a lack of oxidisable organic matter at this depth is unclear. But if iron sulfates are inefficiently reduced by microorganisms, then it is possible that designing expensive reducing wetlands may not be necessary.

Acknowledgments

Funding for this project was provided by a NERC grant (GR9/01923) to K.O.K. and S.H.B. and an Academic Development Fund (No. 329060) from the University of Leeds to K.O.K. We further thank Rob Raiswell for his critical review of the manuscript.

References

- [1] Ivarson, K.C. (1973) Microbiological formation of basic ferric sulfates. *Can. J. Soil Sci.* 53, 315–323.
- [2] Lazaroff, N., Sigal, W. and Wasserman, A. (1982) Iron oxidation and precipitation of ferric hydroxysulfates by resting *Thiobacillus ferrooxidans* cells. *Appl. Environ. Microbiol.* 43, 924–938.
- [3] Norstrom, D.K. (1982) Aqueous pyrite oxidation and the consequent formation of secondary iron minerals. In: *Acid Sulfate Weathering* (Kittrick, J.A., Fanning, D.S., and Hosner, L.R., Eds.), pp. 37–56. Soil Science Society of America, Madison, WI.
- [4] Brady, K.S., Bigham, J.M., Jaynes, W.F. and Logan, T.J. (1986) Influence of sulfate on Fe-oxide formation: Comparisons with a stream receiving acid mine drainage. *Clays Clay Minerals* 34, 266–274.
- [5] Filipek, L.H., Nordstrom, D.K. and Ficklin, W.H. (1987) Interaction of acid mine drainage with waters and sediments of West Squaw Creek in the West Shasta Mining District, California. *Environ. Sci. Technol.* 21, 388–396.
- [6] Bigham, J.M., Schwertmann, U., Carlson, L. and Murad, E. (1990) A poorly crystallized oxyhydroxysulfate of iron formed by bacterial oxidation of Fe(II) in acid mine waters. *Geochim. Cosmochim. Acta* 54, 2743–2758.
- [7] Cornell, R.M., Giovanoli, R. and Schindler, P.W. (1987) Effect of silicate species on the transformation of ferrihydrite into goethite and hematite in alkaline media. *Clays Clay Minerals* 35, 21–28.
- [8] Kleinmann, R.L.P., Crerar, D.A. and Pacelli, R.R. (1981) Biogeochemistry of acid mine drainage and a method to control acid formation. *Min. Eng.* 33, 300–306.
- [9] Chapman, B.M., Jones, D.R. and Jung, R.F. (1983) Processes controlling metal ion attenuation in acid mine drainage streams. *Geochim. Cosmochim. Acta* 47, 1957–1973.
- [10] Carlson, L. and Schwertmann, U. (1980) Natural occurrence of ferroxylite (δ' -FeOOH). *Clays Clay Minerals* 28, 272–280.
- [11] Ivarson, K.C., Ross, G.J. and Miles, N.M. (1979) The microbiological formation of basic ferric sulfates: II. Crystallization in presence of potassium-, ammonium-, and sodium-salts. *Soil Sci. Soc. Am. J.* 43, 908–912.
- [12] Beveridge, T.J., Meloche, J.D., Fyfe, W.S. and Murray, R.J.E. (1983) Diagenesis of metals chemically complexed to bacteria: Laboratory formation of metal phosphates, sulfides, and organic condensates in artificial sediments. *Appl. Environ. Microbiol.* 45, 1094–1108.
- [13] Ferris, F.G., Tazaki, K. and Fyfe, W.S. (1989) Iron oxides in acid mine drainage environments and their association with bacteria. *Chem. Geol.* 74, 321–330.
- [14] Ferris, F.G., Schultze, S., Witten, T.C., Fyfe, W.S. and Beveridge, T.J. (1989) Metal interactions with microbial biofilms in acidic and neutral pH environments. *Appl. Environ. Microbiol.* 55, 1249–1257.
- [15] Konhauser, K.O., Fyfe, W.S., Ferris, F.G. and Beveridge, T.J. (1993) Metal sorption and mineral precipitation by bacteria in two Amazonian river systems: Rio Solimões and Rio Negro, Brazil. *Geology* 21, 1103–1106.
- [16] Konhauser, K.O., Schultze-Lam, S., Ferris, F.G., Fyfe, W.S., Longstaffe, F.J. and Beveridge, T.J. (1994) Mineral precipitation by epilithic biofilms in the Speed River, Ontario, Canada. *Appl. Environ. Microbiol.* 60, 549–553.
- [17] Konhauser, K.O., Fyfe, W.S., Schultze-Lam, S., Ferris, F.G. and Beveridge, T.J. (1994) Iron phosphate precipitation by epilithic microbial biofilms in Arctic Canada. *Can. J. Earth Sci.* 31, 1320–1324.
- [18] Konhauser, K.O. and Ferris, F.G. (1996) Diversity of iron and silica precipitation by microbial mats in hydrothermal waters, Iceland: Implications for Precambrian iron formations. *Geology* 24, 323–326.
- [19] Krom, M.D., Davison, P., Zang, H. and Davison, W. (1994) High-resolution pore-water sampling with a gel sampler. *Limnol. Oceanogr.* 39, 1967–1972.
- [20] Raiswell, R., Canfield, D.E. and Berner, R.A. (1994) A comparison of iron extraction methods for the determination of degree of pyritisation and the recognition of iron-limited pyrite formation. *Chem. Geol.* 111, 101–110.
- [21] Lovley, D.R. (1992) Microbial oxidation of organic matter coupled to the reduction of Fe(III) and Mn(IV) oxides. In: *Biomineralization. Processes of Iron and Manganese* (Skinner, H.C.W. and Fitzpatrick, R.W., Eds.), pp. 101–114. Catena, Cremlingen.
- [22] Ferris, F.G. and Beveridge, T.J. (1986) Site specificity of metallic ion binding in *Escherichia coli* K-12 lipopolysaccharide. *Can. J. Microbiol.* 32, 52–55.
- [23] Brock, T.D., Smith, D.W. and Madigan, M.T. (1984) *Biology of Microorganism*. Prentice-Hall, Englewood Cliffs, NJ.
- [24] Schwertmann, U. and Fitzpatrick, R.W. (1992) Iron minerals in surface environments. In: *Biomineralization. Processes of Iron and Manganese* (Skinner, H.C.W. and Fitzpatrick, R.W., Eds.), pp. 7–30. Catena, Cremlingen.

- [25] Parfitt, R.L. and Smart R.St.C. (1978) The mechanism of sulfate adsorption on iron oxides. *Soil Sci. Soc. Am. J.* 42, 48–50.
- [26] Robinson, G.D. (1981) Adsorption of Cu, Zn and Pb near sulphide deposits by hydrous manganese-iron oxide coatings on stream alluvium. *Chem. Geol.* 33, 65–79.
- [27] Pesavento, B.G. (1987) Factors to be considered in the use of wetlands to treat acid mine drainage. *Environ. Can. Acid. Mine Drainage Symp.* pp. 499–505.
- [28] Pulford, I.D. (1991) A review of methods to control acid generation in pyritic coal mine waste. In: *Land Reclamation* (Davies, M.C.R., Ed.), pp. 269–278. Elsevier, London.
- [29] Machermer, S.D. and Wildeman, T.R. (1992) Adsorption compared with sulfide precipitation as metal removal processes from acid mine drainage in a constructed wetland. *J. Contam. Hydrol.* 9, 115–131.
- [30] Wieder, R.K. (1992) The Kentucky Wetlands Project: A Field Study to Evaluate Man-Made Wetlands for Acid Mine Drainage Treatment. Report to the U.S. Office of Surface Mining, Reclamation and Enforcement.